CONFERENCE PRE-PRINT

DENSITY DEPENDENCE OF CONVECTION IN PARALLEL HEAT TRANSPORT IN THE SCRAPE-OFF LAYER OF JT-60U

R. MATOIKE

Naka Institute for Fusion Science and Technology, National Institutes for Quantum Science and Technology Naka, Ibaraki, Japan

Email: matoike.ryota@qst.go.jp

T. NAKANO

Naka Institute for Fusion Science and Technology, National Institutes for Quantum Science and Technology Naka, Ibaraki, Japan

N. ASAKURA

Naka Institute for Fusion Science and Technology, National Institutes for Quantum Science and Technology Naka, Ibaraki, Japan

R. SANO

Naka Institute for Fusion Science and Technology, National Institutes for Quantum Science and Technology Naka, Ibaraki, Japan

Abstract

The density dependence of the convective parallel heat transport is obtained with reciprocating probes in the Scrape-Off Layer of JT-60U tokamak for the first time. As the line-averaged density increases, the convective contribution increases significantly around the separatrix and exceeds the conductive contribution. As the line-averaged density increases further, the convective contribution exceeds the conductive contribution in the whole radial range. In addition, the power balance among the conductive heat flux, the convective heat flux, and radiated power is discussed. The total power across the probe near the X-point (P_X) is calculated by integrating the radial profile of the conductive and the convective parallel heat flux. As the line-averaged density increases, P_X decreases due to the X-point radiator and radiation losses in the upstream SOL, while the fraction of convection in P_X increases. In contrast, it is found that SONIC modelling does not reproduce the large contribution of the convection in high-density plasmas. These results suggest that another transport model that is not yet implemented in SONIC and that accounts for the large contribution of heat transport by convection is required.

1. INTRODUCTION

Control of heat load onto the divertor target is one of the critical issues in fusion devices. To mitigate the high heat load, a high-density detached divertor operation has been developed, where heat transport characteristics at the Scrape-Off Layer (SOL) are different from those in low-density attached divertor plasmas.

The heat flux parallel to the magnetic field in SOL is transported by conduction and convection. The transport of energy parallel to the magnetic field in the SOL can be described by[1],

$$q_{\parallel} = -\kappa T_{\rm e}^{5/2} \frac{{\rm d}T_{\rm e}}{{\rm d}s} + nv_{\parallel} \left(\frac{5}{2} (T_{\rm i} + T_{\rm e}) + \frac{1}{2} m_{\rm i} v_{\parallel}^2 + I_0 \right) \tag{1}$$

where s is the parallel field line length, κ is the parallel electron thermal conductivity, T_i and T_e are the ion and electron temperatures respectively, n is the plasma density, m_i is the ion mass, ν_{\parallel} is the plasma fluid velocity parallel to the magnetic field, and I_0 is the atomic ionization and molecular potential. The first term in the Equation 1 is electron thermal conduction. The second group of terms in the Equation 1 is convection.

Previous studies show in general that the conductive transport is dominant in low-density SOL plasma and that with increasing density, the convective contribution increases. The quantitative evaluation of conductive parallel heat flux is performed in DIII-D. The parallel heat flux profile is measured with power balance techniques and it is found that the electron temperature gradients are too small to support this heat flux through conduction. The

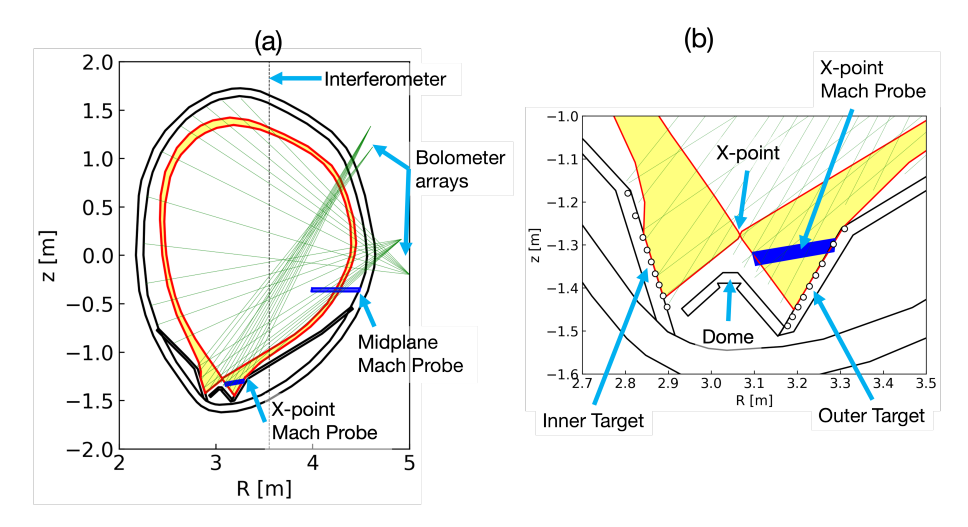


FIG. 1. Plasma cross section and locations of diagnostics

plasma flow profile is infered to supply the remaining heat flux[2, 3, 4]. In JT-60U, measuremnent of SOL flow is performed with multiple reciprocating Mach probes[5, 6, 7, 8]. The electron density dependence of the particle flux is evaluated. However, the density dependence of the conductive and the convective transport contribution, in particular in high-density detached plasmas, is not yet unveiled experimentally. A systematical database of the transport mechanism in the SOL can be a reference for transport model development for future devices.

The paper reports for the first time the density dependence of the convective heat transport contribution in JT-60U attached and detached plasmas in terms of power balance and compare with modelling results. The experimental setup and calculation of parallel heat flux are shown in section 2. In section3, the power balance is discussed and compared with SONIC. Summary and conclusions are given in section 4.

2. EXPERIMENT

A database of NB-heated L-mode dischages on the JT-60U was used for this study. Experiments are performed with plasma current $I_p = 1.6$ MA, troidal magnetic field $B_t = 3.2$ T, and neutral beam heating power $P_{\rm NBI} = 4.0$ MW. The line-averaged electron density $\bar{n}_{\rm e}$ is changed from 1.7×10^{19} to 3.3×10^{19} m⁻³ (Greenwald density fraction $n/n_{\rm GW}$ of 0.18-0.60) on a shot-to-shot basis. The $\bar{n}_{\rm e}$ is measured by the interferometer as shown in Fig.1(a). Eighteen Lagmuir probes mounted at the divertor target measure the Ion saturetion current, electron temperature and electron density at the target(Fig.1(b)). The viewing chords for the bolometer measurement are shown in Fig.1(a) and (b).

The fast reciprocating Lagmuir probe system[9, 5] installed at the outer midplane (M-probe) and below X-point (X-probe) as shown in Fig.1. The electron temperature and density profiles are measured with a spatial resolution of 1-2 mm using double-probe method[5]. The mach number M is also evaluated using Hutchinson's formula[10]. Fig.2 shows typical results of the electron density, electron template and Mach number profiles measured by Langmuir probes in three \bar{n}_e cases.

The parallel conductive and convective heat flux profile along the X-probe are obtaind using Langmuir probe data as follows.

$$q_{\parallel}^{\text{conv}} = \frac{5}{2} \sqrt{\frac{\gamma}{m_{\text{i}}}} M n_{\text{e,X}} T_{\text{e,X}}^{3/2}$$
 (2)

$$q_{\parallel}^{\text{cond}} = \kappa T_{\text{e,X}}^{5/2} \frac{T_{\text{e,M}} - T_{\text{e,X}}}{l_{\parallel,\text{MX}}}$$
 (3)

Here, γ is the heat transmission coefficient, m_i is the ion mass, M is the Mach number, n_e is the electron density, T_e is the electron temperature, κ is the parallel electron thermal conductivity, $l_{\parallel, \rm MX}$ is the connection length between M-probe and X-probe respectively. The subscripts X and M indicate X-probe and M-probe respectively. The convective heat flux $(q_{\parallel}^{\rm conv})$ is obtained using electron temperature, electron density and Mach number measured by X-probe as in Equation 2. The conductive heat flux $(q_{\parallel}^{\rm cond})$ is obtained using electron temperature and parallel gradient of the electron temperature at the X-probe. In this analysis, the ratio of $T_{\rm e,M}-T_{\rm e,X}$ and $t_{\parallel,\rm MX}$ is used to estimate the electron temperature gradient as shown in Equation 3.

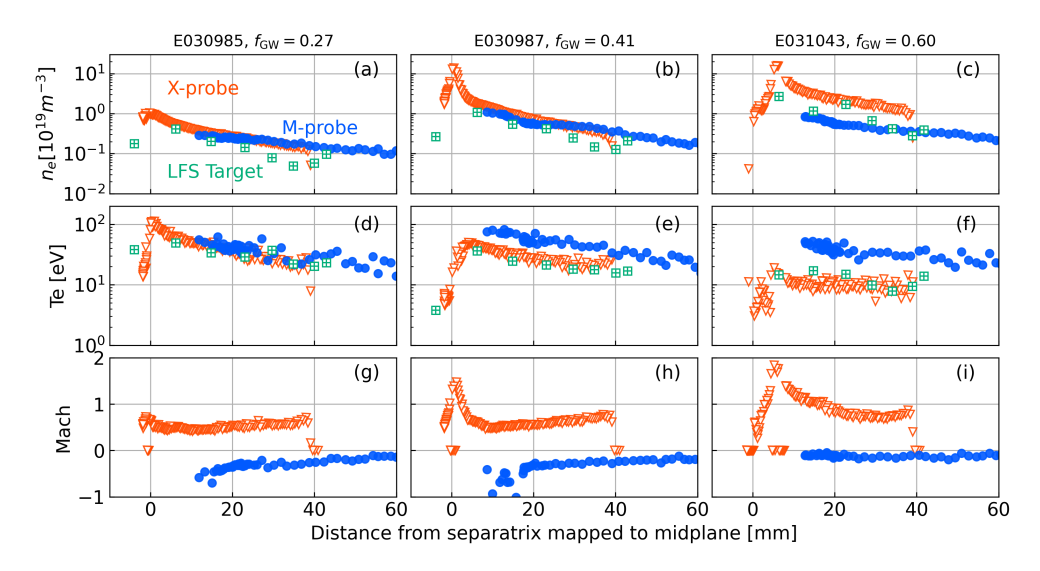


FIG. 2. The radial profiles of the plasma parameters measured by Langmuir Probes are shown. The top, middle, bottom row show the electron density, electron temperature, Mach number respectively. The left, center, right columns show the three density cases respectively; $n/n_{\rm GW}=0.27$, $n/n_{\rm GW}=0.41$, $n/n_{\rm GW}=0.60$.

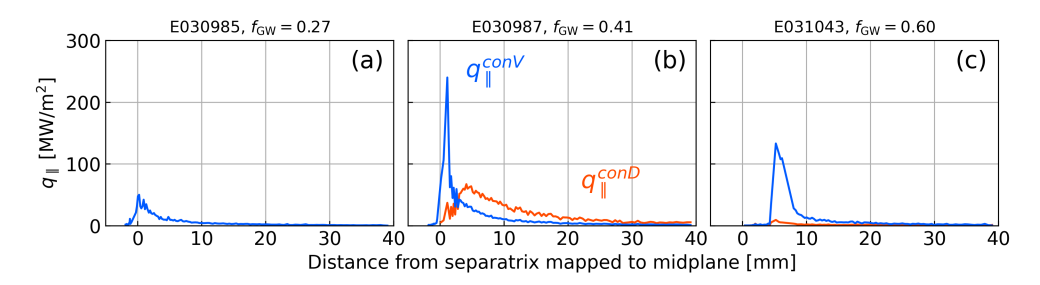


FIG. 3. Radial profile of conductive and convective parallel heat flux along X-probe for (a) $n/n_{\text{GW}} = 0.27$, (b) $n/n_{\text{GW}} = 0.41$, (c) $n/n_{\text{GW}} = 0.60$.

Note that the parallel conductive heat flux is calculated only high-density cases with $n/n_{\rm GW} > 0.4$ because of the higher $T_{\rm e}$ at the divertor than that at midplane in low density cases. This phenomenon could be caused by transport across the separatrix such as $B \times \nabla B$ drift. In Fig.2(b), The convective contribution exceeds the conductive contribution around the separatrix. In contrast, in the distance range larger than 3 mm from the separatrix, the conductive contribution is larger than the convective. As the line-averaged density increases further, the radial width of the convective contribution increases and the convective contribution exceeds the conductive contribution in the whole radial range, including the range far from the separatrix(Fig.2(c)).

3. POWER BALANCE ANALYSIS

The power balance among the conductive heat flux, convective heat flux and radiated power is discussed. Fig.4 (a) shows the power across the X-probe obtained by parallel heat flux shown in Fig.3. The power across the X-probe with conductive transport ($P_X^{\rm ConD}$) and convective transport ($P_X^{\rm ConV}$) is calculated by radial integration of the poloidal component of the $q_{\parallel}^{\rm cond}$ and $q_{\parallel}^{\rm conv}$ respectively. The total power across the X-probe ($P_X^{\rm Prb}$) is obtained by $P_X^{\rm Prb} = P_X^{\rm ConD} + P_X^{\rm ConV}$. As the line-averaged density increases, both of $P_X^{\rm ConD}$ and $P_X^{\rm ConV}$ decreases and the fraction of the convective in $P_X^{\rm Prb}$ increases in range $n/n_{\rm GW} = 0.4 - 0.6$.

The power across the X-probe is also evaluated from the radiation power obtained by bolometers (P_X^{Bol}) to validate the P_X^{Prb} , as shown in Fig.4 (b). P_X^{Bol} is given by,

$$P_{\rm X}^{\rm Bol} = \frac{2}{3} \{ P_{\rm NBI} - (P_{\rm rad}^{\rm Core} + P_{\rm rad}^{\rm XPR}) \} - P_{\rm rad}^{\rm SOL}$$
 (4)

Here, P_{NBI} is the NBI heating power, $P_{\text{rad}}^{\text{Core}}$ is the radiated power in core plasma, $P_{\text{rad}}^{\text{XPR}}$ is the radiated power from X-point radiator, $P_{\text{rad}}^{\text{SOL}}$ is the radiated power at outer SOL upstream of X-probe. In this analysis, it is assumed

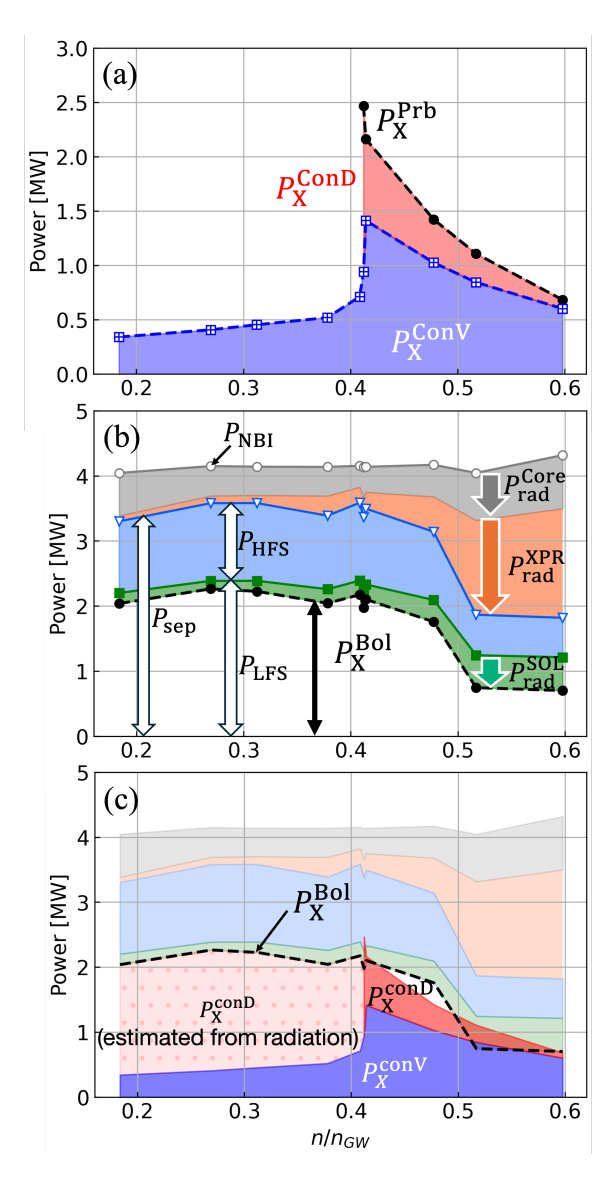


FIG. 4. Electron density dependence of the power across the X-probe obtained by (a) reciprocating Mach probe, (b) NBI injection and radiative power of the bolometer. (c): Comparison of the power across the X-probe obtained in (a) and (b).

that 2/3 of the power flowing across the separatrix to the SOL flowed to low-field side. The $P_{\rm NBI}$ is the deposited power on plasma. Shine through is calculated by OFMC[11] code and deducted from NBI input power. Fig.4 (c) shows the comparison between $P_{\rm X}^{\rm Prb}$ and $P_{\rm X}^{\rm Bol}$. Both of $P_{\rm X}^{\rm Prb}$ and $P_{\rm X}^{\rm Bol}$ decrease from about 2 MW to 0.7 MW in range $n/n_{\rm GW}=0.4-0.6$. The electron density dependence of $P_{\rm X}^{\rm Bol}$ supports $P_{\rm X}^{\rm Prb}$ under current assumptions. The $P_{\rm X}^{\rm ConD}$ in low density cases are estimated to be 1.5 – 1.8 MW from the $P_{\rm X}^{\rm Bol}$ and $P_{\rm X}^{\rm ConV}$.

SONIC code[12], the integrated SOL/divertor code is used to evaluate the electron density dependence of the conductive and convective transport. The electron density scan from attached to detached plasma is simulated by scanning the gas puff rate in range between $1.0 \times 10^{21} \, \mathrm{s^{-1}}$ and $6.0 \times 10^{21} \, \mathrm{s^{-1}}$. The conductive and convective contribution of heat transport at the same position of the X-probe are obtained with the same formulas as in the experiment as shown in Fig.5. In all density cases, including detached plasmas, the contribution from conductive transport exceeds that of convection, and the large contribution of convective transport shown in the experiment is not reproduced. A lower Mach number by SONIC compared with experimental observation is considered to cause the lower convective transport, which is proportional to Mach number as shown in Fig.6. These results suggest that another transport model that is not yet implemented in SONIC and that accounts for the large contribution of heat transport by convection is needed.

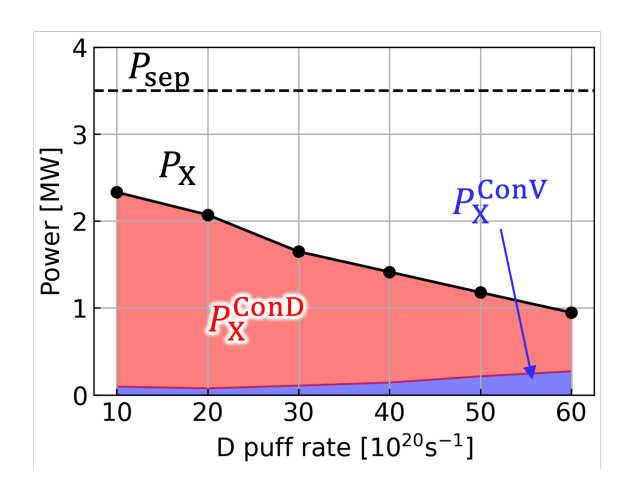


FIG. 5. Electron density dependence of the power across the X-probe obtained by SONIC.

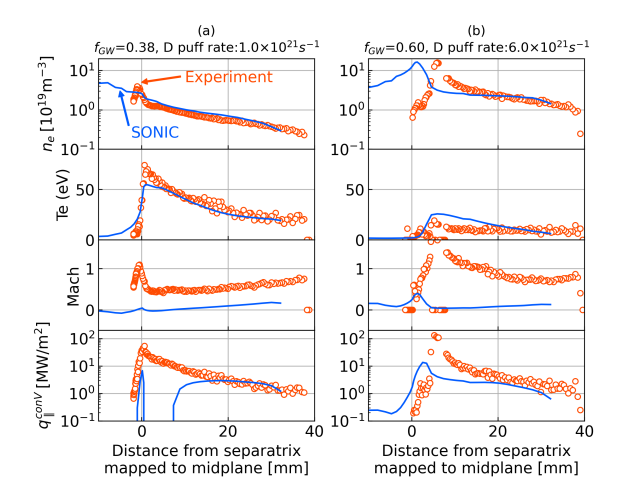


FIG. 6. Comparison between experiment and SONIC

4. CONCLUSIONS

The electron density dependence of the parallel convective transport is quantitatively evaluated in attached and detached plasmas. The conductive contribution is also obtained in high density detached plasmas. The power balance among the conduction, convection and radiation power is discussed. The density dependence of the radiation power supports conduction and convective power across the X-probe. The large contribution of the convection is not reproduced in SONIC.

REFERENCES

- [1] STANGEBY, P. C., *The Plasma Boundary of Magnetic Fusion Devices*, Institute of Physics Publishing, Bristol, U.K., 2000.
- [2] LEONARD, A. W. et al., Distributed Divertor Radiation through Convection in DIII-D, Phys. Rev. Lett. 78 25 (1997) 4769–4772.
- [3] LEONARD, A. W. et al., Radiative divertor plasmas with convection in DIII-D, Physics of Plasmas 5 5 (1998) 1736–1743.
- [4] BOEDO, J. A. et al., Flow reversal, convection, and modeling in the DIII-D divertor, Physics of Plasmas 5 12 (1998) 4305–4310.
- [5] ASAKURA, N. et al., Heat and particle transport of SOL and divertor plasmas in the W shaped divertor on JT-60U, Nucl. Fusion 39 11Y (1999) 1983–1994.
- [6] ASAKURA, N. et al., Measurement of Natural Plasma Flow along the Field Lines in the Scrape-Off Layer on the JT-60U Divertor Tokamak, Phys. Rev. Lett. 84 14 (2000) 3093–3096.
- [7] ASAKURA, N. et al., Driving mechanism of sol plasma flow and effects on the divertor performance in JT-60U, Nucl. Fusion **44** 4 (2004) 503–512.
- [8] ASAKURA, N., Scrape-off Layer Plasma Flow in L- and H-Mode Plasmas on JT-60U, Plasma and Fusion Research 4 (2009) 021–021.
- [9] ASAKURA, N. et al., Fast reciprocating probe system for local scrape-off layer measurements in front of the lower hybrid launcher on JT-60U, Review of Scientific Instruments 66 12 (1995) 5428–5432.
- [10] HUTCHINSON, I. H., Ion collection by probes in strong magnetic fields with plasma flow, Phys. Rev. A **37** 11 (1988) 4358–4366.
- [11] TANI, K. et al., Effect of Toroidal Field Ripple on Fast Ion Behavior in a Tokamak, J. Phys. Soc. Jpn. 50 5 (1981) 1726–1737.
- [12] KAWASHIMA, H. et al., Development of Integrated SOL/Divertor Code and Simulation Study in JAEA, Plasma and Fusion Research 1 (2006) 031–031.